Journal Pre-proofs

Injectable *in situ* forming hydrogels incorporating dual-nanoparticles for chemo-photothermal therapy of breast cancer cells

Ivo J. Sabino, Rita Lima-Sousa, Cátia G. Alves, Bruna L. Melo, André F. Moreira, Ilídio J. Correia, Duarte de Melo-Diogo

PII: S0378-5173(21)00315-X
DOI: https://doi.org/10.1016/j.ijpharm.2021.120510
Reference: IJP 120510

To appear in: *International Journal of Pharmaceutics*

Received Date: 29 December 2020
Revised Date: 3 March 2021
Accepted Date: 17 March 2021

Please cite this article as: I.J. Sabino, R. Lima-Sousa, C.G. Alves, B.L. Melo, A.F. Moreira, I.J. Correia, D. de Melo-Diogo, Injectable *in situ* forming hydrogels incorporating dual-nanoparticles for chemo-photothermal therapy of breast cancer cells, *International Journal of Pharmaceutics* (2021), doi: https://doi.org/10.1016/j.ijpharm.2021.120510

Injectable *in situ* forming hydrogels incorporating dual-nanoparticles for chemo-photothermal therapy of breast cancer cells

Ivo J. Sabino [a], Rita Lima-Sousa [a], Cátia G. Alves [a], Bruna L. Melo [a], André F. Moreira [a], Ilídio J. Correia [a,b,*], Duarte de Melo-Diogo [a,*]

[a] CICS-UBI – Centro de Investigação em Ciências da Saúde, Universidade da Beira Interior, 6200-506 Covilhã, Portugal.

[b] CIEPQPF – Departamento de Engenharia Química, Universidade de Coimbra, 3030-790 Coimbra, Portugal.

* Corresponding authors: Dr. Duarte de Melo-Diogo and Dr. Ilídio J. Correia, Centro de Investigação em Ciências da Saúde, Universidade da Beira Interior, 6200-506 Covilhã, Portugal. E-mail: demelodiogo@fcsaude.ubi.pt and icorreia@ubi.pt

Abstract

Chemo-photothermal therapy (chemo-PTT) mediated by nanomaterials holds a great potential for cancer treatment. However, the tumor uptake of the systemically administered nanomaterials was recently found to be below 1 %. To address this limitation, the development of injectable tridimensional polymeric matrices capable of delivering nanomaterials directly into the tumor site appears to be a promising approach. In this work, an injectable *in situ* forming ionotropically crosslinked chitosan-based hydrogel co-incorporating IR780 loaded nanoparticles (IR/BPN) and Doxorubicin (DOX) loaded nanoparticles (DOX/TPN) was developed for application in breast cancer chemo-PTT. The produced hydrogels (IR/BPN@Gel and IR/BPN+DOX/TPN@Gel) displayed suitable physicochemical properties and produced a temperature increase of about 9.1 °C upon exposure to Near Infrared (NIR) light. As importantly, the NIR-light exposure also increased the release of DOX from the hydrogel by 1.7-times. In the *in vitro* studies, the combination of IR/BPN@Gel with NIR light (photothermal therapy) led to a reduction in the viability of breast cancer cells to 35 %. On the other hand, the non-irradiated IR/BPN+DOX/TPN@Gel (chemotherapy) only diminished cancer cells' viability to 85 %. In contrast, the combined action of IR/BPN+DOX/TPN@Gel and NIR light reduced cancer cells' viability to about 9 %, demonstrating its potential for breast cancer chemo-PTT.

Keywords: Cancer Chemo-Photothermal Therapy, Doxorubicin, Injectable Hydrogel, IR780, Localized Delivery.

1. Introduction

Chemo-photothermal therapy (chemo-PTT) mediated by nanomaterials is a promising modality for treating cancer (Alves et al., 2019; de Melo-Diogo et al., 2018; Li et al., 2018; Nam et al., 2018). This approach explores the ability of systemically administered nanomaterials to accumulate at the tumor site, and the combinatorial effects occurring between the nanomaterials' mediated photoinduced heat and drug delivery (Khafaji et al., 2019; Li et al., 2019b; Liu et al., 2019c; Ye et al., 2019). To trigger the nanomaterials' photothermal effect, the tumor zone is irradiated with near infrared (NIR; 750-1000 nm) light, due to its high tissue penetration depth and minimal interactions with biological components (*e.g.* water, melanin, hemoglobin or collagen) (Rodrigues et al., 2020). Therefore, inorganic nanomaterials with NIR absorption (*e.g.* graphene derivatives (de Melo-Diogo et al., 2018; Leitão et al., 2020a; Liu et al., 2019d), gold nanorods (Moreira et al., 2018; Yang et al., 2017)) or nanostructures encapsulating organic NIR dyes (*e.g.* Indocyanine Green (An et al., 2020; Li et al., 2019a; Ma et al., 2013), IR780 (Liu et al., 2019b; Pais-Silva et al., 2017; Xia et al., 2019), IR808 (Thomas et al., 2018; Xu et al., 2017), IR825 (Pan et al., 2018; Song et al., 2014)) have been the most explored for this type of application. These nanostructures can produce, upon NIR laser irradiation, a temperature increase that damages the cancer cells with minimal off-target heating (Rodrigues et al., 2020). Some NIR-responsive nanomaterials can also encapsulate chemotherapeutic drugs, enabling their use in chemo-PTT (Rodrigues et al., 2020; Zheng et al., 2019a). Alternatively, nanomaterials' mediated chemo-PTT can also be achieved by administrating one nanostructure that loads the chemotherapeutic drug and another that has photothermal capacity (Liu et al., 2019a). This later approach is more straightforward since it is easier to optimize the physicochemical properties (*e.g.* size) of the nanostructures with only one functionality (Liu et al., 2019a). As importantly, the nanomaterials' photoinduced heat can also trigger the release of the encapsulated drugs from the nanomaterials, and increase cancer cells' sensitivity to the chemotherapeutic

drugs, leading to an improved outcome (Khafaji et al., 2019; Li et al., 2019b). Despite of this potential, Wilhelm *et al.* uncovered that less than 1 % of the intravenously administered nanomaterials' dose effectively reaches the tumor site (Wilhelm et al., 2016). In this way, it of utmost importance to develop novel strategies to deliver nanomaterials aimed for chemo-PTT into the tumor site, hence bypassing the systemic administration problems.

In this regard, the delivery of nanomaterials directly into the tumor site by tridimensional (3D) macrostructures (*e.g.* hydrogels, microneedles, or scaffolds) appears to be a promising approach (Alessandri et al., 2019; Carvalho et al., 2018; Huang et al., 2016; Lan et al., 2018; Moreira et al., 2020; Samadi et al., 2018). In particular, injectable *in situ* forming hydrogels hold a great potential for delivering nanomaterials directly into the tumor zone due to their straightforward and readily scalable assembly (Chhibber et al., 2020; Geng et al., 2020; Mathew et al., 2018). In this process, the hydrogel precursor solutions containing the nanomaterials are initially intratumorally administered, achieving gelation at the tumor site (*in situ*) (Chang et al., 2015; Lima-Sousa et al., 2020; Mathew et al., 2018; Peers et al., 2020). Such enables a controlled delivery of high nanomaterial doses into the tumor tissue with minimal systemic exposure (Huang et al., 2016; Norouzi et al., 2016; Ta et al., 2008). For instance, Huang *et al.* produced an injectable poly(ethylene glycol)-poly(caprolactone) based hydrogel with an *in situ* thermoresponsive gelation that could deliver a 7.9-times higher drug dose into the tumor in comparison to systemically administered nanoparticles (Huang et al., 2016). Nevertheless, for this type of application, injectable hydrogels formulated using natural/semi-natural polymers are more appealing due to their excellent biocompatibility and biodegradability (Chhibber et al., 2020; Lee, 2018; Zheng et al., 2019b). Therefore, the formulation of injectable *in situ* forming hydrogels based on natural/semi-natural materials should be pursed for the tumor confined delivery of nanomaterials aimed for chemo-PTT.

In this work, an injectable *in situ* forming ionotropically crosslinked chitosan-based hydrogel co-incorporating IR780 loaded bovine serum albumin (BSA) polymeric nanoparticles (IR/BPN) and Doxorubicin (DOX) loaded D-α-tocopheryl polyethylene glycol 1000 succinate (TPGS) polymeric nanoparticles (DOX/TPN) was prepared (IR/BPN+DOX/TPN@Gel), for the first time, to be applied in cancer chemo-PTT. Chitosan was selected due to its good biocompatibility and biodegradability as well as due to its gelation in the presence of $NaHCO_3$ (Miguel et al., 2014; Ta et al., 2008; Wang et al., 2019b). In order to endow the hydrogel with photothermal capabilities, IR/BPN were incorporated within the 3D polymeric network due to the excellent optical properties of IR780, which are superior or similar to those of other NIR-responsive dyes (*e.g.* Indocyanine Green and IR808) (Leitão et al., 2020b). Furthermore, BSA-based nanomaterials also display an excellent loading capacity (Elzoghby et al., 2012). In turn, to include the chemotherapeutic function in the hydrogel, DOX/TPN were also incorporated due to the DOX' broad spectrum chemotherapeutic activity and TPGS' amphiphilic character (Shafei et al., 2017; Yang et al., 2018).

2. Materials and Methods

2.1. Materials

BSA was bought from Amresco (Pennsylvania, USA). Chitosan low molecular weight (50 000 – 190 000 Da), DL-dithiothreitol (DTT), Dulbecco's Modified Eagle's Medium F12 (DMEM-F12), IR780 iodide, Phosphate Buffered Saline (PBS), resazurin, TPGS and trypsin were purchased from Sigma-Aldrich (Sintra, Portugal). Acetone, methanol and $NaHCO_3$ were purchased from Fisher Scientific (Oeiras, Portugal). Cell culture plates and T-flasks were acquired from Thermo Fisher Scientific (Porto, Portugal). DOX was obtained from Carbosynth (Berkshire, UK). Lysozyme from chicken egg was acquired from Alfa Aesar (Haverhill, MA, USA). Fetal Bovine Serum (FBS) was provided by

Biochrom AG (Berlin, Germany). Michigan Cancer Foundation-7 (MCF-7) cell line and Normal Human Dermal Fibroblast (NHDF) were obtained from ATCC (Middlesex, UK) and Promocell (Heidelberg, Germany), respectively. Water used in all experiments was double deionized (0.22 μm; 18.2 MΩ cm^{-1}).

2.2. Methods

2.2.1. Formulation of IR/BPN and DOX/TPN

The IR/BPN were prepared by adapting a nanoprecipitation method previously described by our group (Alves et al., 2020). Briefly, BSA (5 mg) and DTT (386 μg) were allowed to react for 20 min, under stirring, in 5 mL of PBS. Afterwards, IR780 (250 μg, in 1 mL of acetone) was added dropwise into the BSA-DTT solution, under constant stirring, for 2 h at room temperature. The obtained solution was recovered, dialyzed against water for 90 min (14 000 Da molecular weight cut-off membrane), and filtered (0.45 μm pore size), yielding IR/BPN. As control, blank BSA polymeric nanoparticles (BPN) were also produced as described above without the IR780 addition step.

The DOX/TPN were prepared as we have previously described (Pais-Silva et al., 2017). Briefly, a mixture of TPGS (5 mg) and DOX (250 μg) in 1 mL of acetone was prepared, and it was added dropwise into 5 mL of water, under constant stirring, for 2 h at room temperature. The obtained solution was recovered, dialyzed against water for 90 min (500 – 1 000 Da molecular weight cut-off membrane), and filtered (0.45 μm pore size), yielding DOX/TPN.

2.2.2. Physicochemical characterization of IR/BPN and DOX/TPN

The IR/BPN and DOX/TPN size distribution (at a scattering angle of 173°) and zeta potential were evaluated in a Zetasizer Nano ZS (Malvern Instruments Ltd., Worcestershire, UK). The Vis-NIR absorption spectrum of IR/BPN and DOX/TPN was

also acquired (Evolution 201 UV–Visible spectrophotometer (Thermo Fisher Scientific Inc., Massachusetts, USA)).

To determine the IR780 content in IR/BPN, these nanoparticles were freeze-dried (Canvas CoolSafe, Labo-Gene ApS, Lynge, Denmark) and then resuspended in 1 mL of water:methanol (1:1 (v/v)). Afterwards, a standard curve of IR780 (in 1:1 (v/v) water:methanol) and the absorbance of the IR/BPN sample at 780 nm were used to determine the content of IR780 (Mó et al., 2020). To determine the DOX content in DOX/TPN, these nanoparticles were also freeze-dried and resuspended in 1 mL of methanol. Then, a standard curve of DOX (in methanol) and the DOX/TPN absorbance at 485 nm were used to assess the DOX content. Then, the encapsulation efficiency of IR780 in IR/BPN and of DOX in DOX/TPN were determined as previously described (Pais-Silva et al., 2017).

2.2.3. Preparation of the ionotropically crosslinked chitosan-based hydrogels

The injectable *in situ* forming ionotropically crosslinked chitosan-based hydrogel incorporating IR/BPN (IR/BPN@Gel) was prepared by adapting the method described by Wang *et al.* (Wang et al., 2019b). Firstly, the gelling agent solution was prepared by dissolving $NaHCO_3$ (945 mg) in PBS (0.1 M, 20 mL). Then, the gelling agent solution (200 µL) was mixed with IR/BPN (400 µL; 35 µg mL^{-1} of IR780 equivalents). Afterwards, this solution was added to the chitosan solution (900 µL; 4 % (w/v) in HCl). Subsequently, the gelling agent-IR/BPN-chitosan solution was loaded into a syringe and it was extruded (400 µL *per* template) into hollow cylindrical and removable templates (⌀ = 8 mm; height = 4 mm) in order to attain hydrogels with uniform macroscopic features. This hydrogel formulation was stored at physiological-like conditions (37 °C, 5 % CO_2) before its use. As a control, injectable *in situ* forming ionotropically crosslinked chitosan hydrogels were also prepared with blank (non-drug loaded) BPN (termed as Gel).

For the preparation of the IR/BPN+DOX/TPN@Gel, a similar protocol was used, with slight alterations. Briefly, a mixture of the gelling agent (200 µL), IR/BPN (400 µL; 35 µg mL^{-1} of IR780 equivalents) and DOX/TPN (200 µL; 15 µg mL^{-1} of DOX equivalents) was prepared and added to the chitosan solution (900 µL; 4 % (w/v) in HCl). Then, the gelling agent-IR/BPN-DOX/TPN-chitosan solution was loaded into a syringe and it was extruded (400 µL *per* template) as described above.

2.2.4. Characterization of the Gel, IR/BPN@Gel and IR/BPN+DOX/TPN@Gel

The swelling behavior of the hydrogels was determined following a protocol previously described (Lima-Sousa et al., 2020). Briefly, Gel, IR/BPN@Gel and IR/BPN+DOX/TPN@Gel were immersed in a PBS solution (pH 7.4) at 37 °C, under stirring. At predetermined timepoints, the hydrogels were removed from the PBS solution and weighted. Afterwards, they were immersed in a new PBS solution. The swelling ratio was determined using the following equation (W_F and W_I represent the weight of the hydrogels at the determined timepoints and at the beginning, respectively):

$$\text{Swelling Ratio}\ (\%) = \frac{W_F - W_I}{W_I} \times 100 \quad (1)$$

The degradation of Gel, IR/BPN@Gel and IR/BPN+DOX/TPN@Gel in biologically mimicking conditions was also investigated (Cabral et al., 2019). For such, each hydrogel was placed in a PBS solution (pH 7.4, 1 mL) containing lysozyme (13.6 mg L^{-1}) at 37 °C, under stirring for 7 days. The PBS-enzyme solution was replaced every 2 days. At predetermined timepoints, the hydrogels were recovered and washed 3 times with water, freeze-dried and then weighted. The weight loss at the determined timepoints was calculated according to the following equation (W_I and W_T represent the hydrogels' initial weight and the hydrogels' weight at time t, respectively):

$$\text{Weight Loss}\ (\%) = \frac{W_I - W_T}{W_I} \times 100 \quad (2)$$

The cross-section morphology of Gel, IR/BPN@Gel and IR/BPN+DOX/TPN@Gel was observed by Scanning Electron Microscopy (SEM) at an acceleration voltage of 20 kV using a Hitachi S-3400N Scanning Electron Microscope (Japan).

The rheological characterization of the produced hydrogels was performed in a Thermostated Brookfield DV3T cone-plate rheometer using a CP52Z cone ((Brookfield Ametek, Massachusetts, USA), with a sample volume of 500 µL. All the experiments were carried out at 37 °C. The apparent viscosity of the hydrogels was determined at increasing shear rates (60-340 s^{-1}) and it was also analyzed as a function of time (30 min of total time; constant speed of 60 rpm). Throughout the assays, the results were not considered when the torque value was superior to 95%.

The photothermal capacity of Gel, IR/BPN@Gel and IR/BPN+DOX/TPN@Gel was also analyzed (Alves et al., 2019; Lima-Sousa et al., 2020). For this purpose, the hydrogels were immersed in water and then irradiated with NIR light for 10 min (808 nm, 1.7 W cm^{-2}). At predetermined timepoints, the temperature variations were recorded using a thermocouple thermometer. As control, water (without any hydrogel) was also irradiated and the attained temperature variations recorded.

The release profile of DOX from the IR/BPN+DOX/TPN@Gel was determined by placing this formulation in a PBS solution containing lysozyme (pH 7.4, 13.6 mg L^{-1}) at 37 °C (Lima-Sousa et al., 2020). At pre-established timepoints, the PBS-enzyme solution was recovered and replaced by a fresh one. Afterwards, the DOX content in the recovered solutions was determined by absorption spectroscopy. The influence of the NIR light exposure on the release of DOX was also assessed by irradiating the hydrogel (808 nm, 1.7 W cm^{-2}, 10 min).

For analyzing the long-term stability of Gel, IR/BPN@Gel and IR/BPN+DOX/TPN@Gel, their respective precursor solutions (described in Section 2.2.3.) were stored at 4 °C, during 7 days. Afterwards, the hydrogels were assembled by loading the stored solutions

into syringes. Then, the injectability and gelation after storage were evaluated. The size distribution of the IR/BPN and DOX/TPN after storage was also evaluated.

2.2.5. Evaluation of Gel and IR/BPN@Gel cytocompatibility

The cytocompatibility of Gel and IR/BPN@Gel (3.73 μg mL^{-1} of IR780 equivalents) was evaluated on MCF-7 cells (breast cancer cell model) and NHDF (normal cell model) using the resazurin method (Lima-Sousa et al., 2020). For the cell culture assays, both cell lines were cultured in DMEM-F12 supplemented with 10 % (v/v) of FBS and 1 % (v/v) of penicillin/streptomycin, in a humidified incubator (37 °C, 5 % CO_2). Briefly, 2×10^4 cells/well were seeded in 12-well plates. After 24 h, the culture medium was removed, and the cells were incubated with fresh medium and with the Gel or IR/BPN@Gel. After 24 or 48 h of incubation, the hydrogels were removed, and the cells were incubated with fresh culture medium containing resazurin (10 % (v/v)) for 4 h in the dark (37 °C, 5 % CO_2). Then, the fluorescence of resorufin (λ_{ex} = 560 nm; λ_{em} = 590 nm) was measured (Spectramax Gemini EM spectrofluorometer, Molecular Devices LLC, CA, USA) to determine the cells' viability. Cells solely incubated with medium and ethanol (70 % (v/v)) were used as negative (K^-) and positive (K^+) controls, respectively.

2.2.6. *In vitro* evaluation of the PTT mediated by IR/BPN@Gel and of the chemo-PTT mediated by IR/BPN+DOX/TPN@Gel

The therapeutic effect mediated by IR/BPN@Gel and IR/BPN+DOX/TPN@Gel was determined using the resazurin method as described above. Initially, MCF-7 cells were seeded as described in Section 2.2.5. After 24 h, cells were incubated with fresh medium and with IR/BPN@Gel (3.73 μg mL^{-1} of IR780 equivalents) or IR/BPN+DOX/TPN@Gel (3.29/0.71 μg mL^{-1} of IR780/DOX equivalents). Then, after 4 h of incubation, the hydrogels were irradiated with NIR light (808 nm, 1.7 W cm^{-2}, 10 min). Subsequently,

after totaling 24 h of incubation, the cells' viability was evaluated as described in Section 2.2.5.

2.2.7. Statistical Analysis

To compare multiple groups, a one-way Analysis of Variance (ANOVA) with the Student-Newman-Keuls test was used. A value of p lower than 0.05 ($^{*}\ p < 0.05$) was considered statistically significant. All data are represented as the mean ± Standard Deviation (S.D.). Data analysis was performed in the GraphPad Prism v6.0 Software (trial version, GraphPad Software, CA, USA).

3. Results and Discussion

3.1. Formulation and characterization of IR/BPN and DOX/TPN

The incorporation of IR/BPN and DOX/TPN in the injectable *in situ* forming ionotropically crosslinked chitosan hydrogel enables their application in cancer chemo-PTT (Figure 1A).

Therefore, IR/BPN and DOX/TPN were initially prepared using a nanoprecipitation method. The Dynamic Light Scattering analysis demonstrated that IR/BPN presented an average size of 89.4 ± 1.0 nm while the DOX/TPN showed a size of 56.3 ± 0.5 nm (n = 3; batch triplicates; Figure S1A). The smaller size of DOX/TPN is related with the ability of TPGS to assemble into very small nanostructures (Nguyen et al., 2016; Yang et al., 2018). Nevertheless, the size of both IR/BPN and DOX/TPN is within the dimensions considered as ideal for cancer related applications (Durymanov et al., 2019; Stern et al., 2017; Wang et al., 2012). For instance, Stern *et al.* demonstrated that nanoparticles with a mean size of 50-90 nm have a good penetration into 3D tumor-like cellular aggregates, as well as a suitable uptake by cancer cells (Stern et al., 2017).

The zeta potential of IR/BPN and DOX/TPN were -4.8 ± 0.5 mV and -4.1 ± 0.5 mV, respectively. In this way, these nanoformulations have a surface charge within the so-called neutral surface charge range (zeta potential between -10 and +10 mV), which has been considered as optimal for tumor penetration (Rodrigues et al., 2020). Furthermore, the surface charge of IR/BPN and DOX/TPN is also in line with that reported in the literature for BSA-based and TPGS-based nanomedicines (Ferrado et al., 2019; Liu et al., 2016).

Then, the absorption of IR/BPN and DOX/TPN was analyzed (Figure S1B). As expected, the IR/BPN exhibited a peak at 791 nm (Figure S1B), which is characteristic of encapsulated IR780 (Alves et al., 2020; Mó et al., 2020). In turn, the DOX/TPN displayed the characteristic absorption peak of DOX at 485 nm (Moreira et al., 2014). The IR/BPN displayed an IR780 encapsulation efficiency of 72.4 ± 2.9 %. On the other hand, the DOX/TPN encapsulated DOX with an efficiency of about 43.3 ± 3.7 %. The lower encapsulation capacity of DOX/TPN may be related with their smaller sized hydrophobic core (Guo et al., 2013). Nevertheless, these encapsulation results are in agreement with those previously reported for other BSA- and TPGS-based nanoparticles (Arora et al., 2017; Pan and Feng, 2008).

3.2. Preparation and characterization of Gel, IR/BPN@Gel and IR/BPN+DOX/TPN@Gel

After the preparation of IR/BPN and DOX/TPN, these nanoformulations were added to chitosan and $NaHCO_3$, for the assembly of the injectable *in situ* forming ionotropically crosslinked hydrogels with chemo-photothermal capacity (Figure 1A). For such, a mixture of IR/BPN, DOX/TPN, $NaHCO_3$, and chitosan was loaded into a syringe and was injected into hollow cylindrical and removable templates. Such led to the assembly of individual IR/BPN+DOX/TPN@Gel with uniform macroscopic characteristics for the subsequent assays (Figure S2A). Hydrogels incorporating only IR/BPN were also

prepared using the same procedure (termed as IR/BPN@Gel). As a control, hydrogels with blank (non-loaded) BPN were also produced (termed as Gel). All the three different formulations displayed consistent macroscopic characteristics (Figure S2A) and an irregular-interconnected porous inner structure (Figure S2B). Compared to Gel, the IR/BPN@Gel and IR/BPN+DOX/TPN@Gel displayed a more cohesively packed inner structure, which could result from the ability of the nanoparticles to establish interactions with the hydrogels' polymeric network (Mathew et al., 2018; Merino et al., 2015).

Subsequently, the swelling behavior of the different hydrogels was investigated (Figure 1B). The three formulations exhibited similar swelling profiles, reaching a maximum swelling of about 13 % after 24 h of incubation (Figure 1B). The slow swelling exhibited by these hydrogels is of utmost importance since an abrupt and high swelling profile would compromise the future application on these hydrogels inside tumoral mass (Singh et al., 2016).

Then, the hydrogels' degradability in biologically mimicking conditions was analyzed (Figure 1C). In general, all hydrogel formulations displayed an initial weight loss of 17 % after 1 day of incubation. The Gel formulation achieved its maximum weight loss of about 24 %, after 3 days of incubation (Figure 1C). In stark contrast, both IR/BPN@Gel and IR/BPN+DOX/TPN@Gel displayed an incubation time-dependent weight loss, having their mass decreased by about 48 % by day 7 (Figure 1C). In this way, the sustained degradability of IR/BPN@Gel and IR/BPN+DOX/TPN@Gel may enable a controlled release of the different nanoformulations.

The apparent viscosity of Gel, IR/BPN@Gel and IR/BPN+DOX/TPN@Gel decreased with the increment of the applied shear rate (Figure S3A), displaying a non-Newtonian behavior (Lima-Sousa et al., 2020; Szyma□ska et al., 2015). Furthermore, the viscosity of all the formulations increased along time, which is crucial for their *in situ* gelation after injection (Figure S3B). These behaviors are in line with those displayed by other

chitosan-based hydrogels (Khodaverdi et al., 2012; Lima-Sousa et al., 2020; Szyma□ska et al., 2015).

Afterwards, the photothermal capacity of the hydrogels was assessed by exposing them to NIR radiation during a period of 10 min (808 nm, 1.7 W cm^{-2}) – Figure 1D. The IR/BPN@Gel and IR/BPN+DOX/TPN@Gel produced an irradiation time-dependent photoinduced heat. After 10 min of NIR laser irradiation, the IR/BPN@Gel (3.73 μg mL^{-1} of IR780 equivalents) and IR/BPN+DOX/TPN@Gel (3.29 μg mL^{-1} of IR780 equivalents) produced a temperature increase of 9.2 °C and 9.0 °C, respectively (Figure 1D). The photothermal capacity of these hydrogels is related with the presence of IR/BPN in their structure (Alves et al., 2020). As importantly, such temperature increase can cause damage to cells, leading to a therapeutic effect (Gai et al., 2018; Wang et al., 2019a). As expected, the irradiation of Gel with NIR light did not cause a meaningful temperature variation since this formulation does not have any photothermal nanoagent within its matrix (Figure 1D). Similarly, water (control) exposed to NIR light also did not suffer any significant temperature variation, which is in concordance with its weak/minimal interaction with 808 nm light (Rodrigues et al., 2020). As importantly, the NIR laser irradiation also increased the DOX release from the IR/BPN+DOX/TPN@Gel by up to 1.7-fold (Figure 1E). In this way, IR/BPN+DOX/TPN@Gel may be able to promote an on-demand therapeutic effect.

Wang *et al.* developed alginate-based hydrogels incorporating iodine-starch complexes (1 mg mL^{-1}) that produced a temperature increase of 19.4 °C after NIR light exposure (808 nm, 2.0 W cm^{-2}, 10 min) (Wang et al., 2019a). In another work, Lima-Sousa *et al.* verified that chitosan-agarose hydrogels incorporating reduced graphene oxide produce a photoinduced heat of 8.1 °C (10 μg mL^{-1}; 808 nm, 1.7 W cm^{-2}, 10 min) (Lima-Sousa et al., 2020). Herein, the IR/BPN+DOX/TPN@Gel was able to induce a temperature increase of 9.0 °C using a lower dose of photothermal nanoagent (3.29 μg mL^{-1} of IR780

equivalents) and using a lower/similar NIR radiation intensity (1.7 W cm^{-2}). These findings attest the good photothermal capacity of IR/BPN+DOX/TPN@Gel.

Finally, the long-term stability of the different hydrogels was evaluated. After 7 days of storage at 4 °C, the IR/BPN and DOX/TPN did not suffer any aggregation and thus retained most of their original size distribution (Figure S4). Furthermore, by loading the stored nanoformulations and the stored hydrogels' precursor solutions ($NaHCO_3$ and chitosan solutions) into a syringe, the injectability and gelation of the different hydrogels were still achieved (Figure S5), thus demonstrating a good stability.

Taken together, these results demonstrate the good physicochemical and optical properties of IR/BPN@Gel and IR/BPN+DOX/TPN@Gel.

3.3. Evaluation of Gel and IR/BPN@Gel cytocompatibility

Then, the cytocompatibility of the Gel and IR/BPN@Gel towards MCF-7 and NHDF cells was assessed (Figure 2). Both hydrogel formulations revealed a cytocompatible profile towards both breast cancer and healthy cells, even after 48 h of incubation (viability > 86 %) – Figure 2. The good cytocompatibility of the Gel and IR/BPN@Gel is related with the excellent biocompatibility of chitosan-based hydrogels (Hamedi et al., 2018; Miguel et al., 2014; Peers et al., 2020). In fact, Lima-Sousa *et al.* also demonstrated the good cytocompatible profile of injectable *in situ* forming chitosan-agarose hydrogels (Lima-Sousa et al., 2020). Moreover, non-irradiated IR780 based nanomedicines are also generally cytocompatible (Kuang et al., 2017; Lin et al., 2018; Song et al., 2019). Together, these results confirm the good cytocompatibility of the IR/BPN@Gel.

3.4. *In vitro* evaluation of the PTT mediated by IR/BPN@Gel and chemo-PTT mediated by IR/BPN+DOX/TPN@Gel

Then, the therapeutic effect mediated by IR/BPN@Gel and IR/BPN+DOX/TPN@Gel towards MCF-7 cells was investigated. For such, cells were incubated with the hydrogel formulations and exposed to NIR light (808 nm, 1.7 W cm^{-2}, 10 min) – Figure 3A.

MCF-7 cells incubated with IR/BPN@Gel and exposed to NIR light experienced a reduction in their viability to about 35 % (Figure 3B). Such effect is related with the ability of the IR/BPN incorporated on this hydrogel to produce a photoinduced heat that can damage the cancer cells (Figure 1D). As expected, cells solely incubated with IR/BPN@Gel or solely exposed to NIR light did not suffer any meaningful variation in their viability (Figure 3B). These results are justified by the good cytocompatible profile displayed by IR/BPN@Gel (Figure 2A) and by the negligible off-targeting heating of water exposed to NIR light, respectively (Figure 1D).

Xie *et al.* developed an agarose-based hydrogel incorporating black phosphorus nanosheets that, when irradiated with NIR light (0.5 mg mL^{-1} of black phosphorus nanosheets; 808 nm, 0.925 W cm^{-2}, 10 min), induced a reduction in cancer cells' viability to 39 % (Xie et al., 2020). Herein, the IR/BPN@Gel induced a similar reduction in the cancer cells' viability at an extremely lower dose of the photothermal nanoagent (3.73 µg mL^{-1} of IR780 equivalents) but at a higher laser intensity (1.7 W cm^{-2}). These results attest the potential of IR/BPN@Gel for cancer PTT.

On the other hand, 85 % of the MCF-7 cells incubated with IR/BPN+DOX/TPN@Gel (3.29/0.71 µg mL^{-1} of IR780/DOX equivalents) remained viable. However, when the cells were exposed to IR/BPN+DOX/TPN@Gel plus NIR light, their viability suffered a stark decrease to 9 % (Figure 3B). In this way, the improved therapeutic outcome attained by conjugating IR/BPN+DOX/TPN@Gel with NIR light is explained by the combined action

of the chemo-photothermal effect and by the NIR-light enhanced DOX release (Figure 1E).

Jiang *et al.* prepared a poly(ethylene glycol)-based hydrogel incorporating palladium nanosheets and DOX that, after NIR-light exposure (60/1 μg mL^{-1} of palladium/DOX; 808 nm, 0.6 W cm^{-2}, 10 min), reduced the cancer cells' viability to about 20 % (Jiang et al., 2020). In another study, injectable *in situ* forming chitosan-agarose hydrogels incorporating reduced graphene oxide (10 μg mL^{-1}) and a DOX:Ibuprofen combination (90.4 μM of the 1:5 DOX:Ibuprofen combination) could decrease MCF-7 cells' viability to 34 % after irradiation with NIR light (808 nm, 1.7 W cm^{-2}, 10 min) (Lima-Sousa et al., 2020). Herein, the chemo-PTT mediated by IR/BPN+DOX/TPN@Gel diminished the MCF-7 cells' viability to only 9 %, using a very low dose of therapeutic nanoagents (3.29/0.71 μg mL^{-1} of IR780/DOX equivalents) and at a similar/higher radiation intensity (1.7 W cm^{-2}). In this way, the IR/BPN+DOX/TPN@Gel is a promising injectable *in situ* forming hydrogel that has potential for being applied in the chemo-PTT of breast cancer.

4. Conclusion

In this work, an injectable *in situ* forming ionotropically crosslinked chitosan-based hydrogel co-incorporating IR/BPN and DOX/TPN was prepared, for the first time, for application in cancer chemo-PTT. The obtained results revealed that IR/BPN@Gel and IR/BPN+DOX/TPN@Gel present suitable physicochemical properties to be used in cancer therapy. Upon NIR light exposure, the IR/BPN@Gel and IR/BPN+DOX/TPN@Gel produced a temperature increase of 9.2 °C and 9.0 °C, respectively, confirming their photothermal capacity. As importantly, the NIR-light exposure also increased the release of DOX from the hydrogel by 1.7-times. In the *in vitro* studies, the IR/BPN@Gel presented a cytocompatible behavior towards breast cancer and normal cells. Moreover, the combination of IR/BPN@Gel with NIR light

(photothermal therapy) led to a reduction in the viability of breast cancer cells to 35 %. On the other hand, the non-irradiated IR/BPN+DOX/TPN@Gel (chemotherapy) only diminished cancer cells' viability to 85 %. In stark contrast, the chemo-PTT mediated by IR/BPN+DOX/TPN@Gel reduced the cancer cells' viability to about 9 %. Overall, these results demonstrate that IR/BPN+DOX/TPN@Gel is an injectable *in situ* forming hydrogel with great potential for the chemo-PTT of breast cancer cells.

In the future, it will be interesting to assess the chemo-photothermal effect of IR/BPN+DOX/TPN@Gel in *in vivo* studies as well as the hydrogel's biocompatibility and biodegradability. Moreover, the continuous development of macroscale delivery strategies to address the nanostructures' systemic administration problems will pave the way for the broader clinical application of nanomaterials in cancer therapy.

Acknowledgments: This work was financed by the Foundation for Science and Technology (FCT), through funds from the State Budget, and by the European Regional Development Fund (ERDF), under the Portugal 2020 Program, through the Regional Operational Program of the Center (Centro 2020), through the Project with the reference UIDB/00709/2020. The funding from CENTRO-01-0145-FEDER-028989 and POCI-01-0145-FEDER-031462 is also acknowledged. Duarte de Melo-Diogo acknowledges CENTRO-01-0145-FEDER-028989 for the funding given on the form of a research contract. Rita Lima-Sousa and Cátia G. Alves acknowledge individual PhD fellowships from FCT (SFRH/BD/144922/2019 and SFRH/BD/145386/2019).

Declarations of interest: none.

5. References

Alessandri, G., Coccè, V., Pastorino, F., Paroni, R., Dei Cas, M., Restelli, F., Pollo, B., Gatti, L., Tremolada, C., Berenzi, A., 2019. Microfragmented human fat tissue is a natural scaffold for drug delivery: Potential application in cancer chemotherapy. Journal of Controlled Release 302, 2-18. 10.1016/j.jconrel.2019.03.016.

Alves, C.G., de Melo-Diogo, D., Lima-Sousa, R., Correia, I.J., 2020. IR780 loaded sulfobetaine methacrylate-functionalized albumin nanoparticles aimed for enhanced breast cancer phototherapy. International Journal of Pharmaceutics 582, 1-9. 10.1016/j.ijpharm.2020.119346.

Alves, C.G., de Melo-Diogo, D., Lima-Sousa, R., Costa, E.C., Correia, I.J., 2019. Hyaluronic acid functionalized nanoparticles loaded with IR780 and DOX for cancer chemo-photothermal therapy. European Journal of Pharmaceutics and Biopharmaceutics 137, 86-94. 10.1016/j.ejpb.2019.02.016.

An, F., Yang, Z., Zheng, M., Mei, T., Deng, G., Guo, P., Li, Y., Sheng, R., 2020. Rationally assembled albumin/indocyanine green nanocomplex for enhanced tumor imaging to guide photothermal therapy. Journal of Nanobiotechnology 18, 1-11. 10.1186/s12951-020-00603-8.

Arora, D., Kumar, A., Gupta, P., Chashoo, G., Jaglan, S., 2017. Preparation, characterization and cytotoxic evaluation of bovine serum albumin nanoparticles encapsulating 5-methylmellein: A secondary metabolite isolated from *Xylaria psidii*. Bioorganic & Medicinal Chemistry Letters 27, 5126-5130. 10.1016/j.bmcl.2017.10.064.

Cabral, C.S., Miguel, S.P., de Melo-Diogo, D., Louro, R.O., Correia, I.J., 2019. Green reduced graphene oxide functionalized 3D printed scaffolds for bone tissue regeneration. Carbon 146, 513-523. 10.1016/j.carbon.2019.01.100.

Carvalho, S.M., Mansur, A.A., Capanema, N.S., Carvalho, I.C., Chagas, P., de Oliveira, L.C.A., Mansur, H.S., 2018. Synthesis and in vitro assessment of anticancer hydrogels composed by carboxymethylcellulose-doxorubicin as potential transdermal delivery systems for treatment of skin cancer. Journal of Molecular Liquids 266, 425-440. 10.1016/j.molliq.2018.06.085.

Chang, G., Chen, Y., Li, Y., Li, S., Huang, F., Shen, Y., Xie, A., 2015. Self-healable hydrogel on tumor cell as drug delivery system for localized and effective therapy. Carbohydrate Polymers 122, 336-342. 10.1016/j.carbpol.2014.12.077.

Chhibber, T., Shinde, R., Lahooti, B., Bagchi, S., Varahachalam, S.P., Gaddam, A., Jaiswal, A.K., Gracia, E., Chand, H.S., Kaushik, A., 2020. Hydrogels in Tissue Engineering, Intelligent Hydrogels in Diagnostics and Therapeutics. CRC Press, pp. 105-122.

de Melo-Diogo, D., Costa, E.C., Alves, C.G., Lima-Sousa, R., Ferreira, P., Louro, R.O., Correia, I.J., 2018. POxylated graphene oxide nanomaterials for combination chemo-phototherapy of breast cancer cells. European Journal of Pharmaceutics and Biopharmaceutics 131, 162-169. 10.1016/j.ejpb.2018.08.008.

Durymanov, M., Kroll, C., Permyakova, A., Reineke, J., 2019. Role of Endocytosis in Nanoparticle Penetration of 3D Pancreatic Cancer Spheroids. Molecular Pharmaceutics 16, 1074-1082. 10.1021/acs.molpharmaceut.8b01078.

Elzoghby, A.O., Samy, W.M., Elgindy, N.A., 2012. Albumin-based nanoparticles as potential controlled release drug delivery systems. Journal of Controlled Release 157, 168-182. 10.1016/j.jconrel.2011.07.031.

Ferrado, J.B., Perez, A.A., Visentini, F.F., Islan, G.A., Castro, G.R., Santiago, L.G., 2019. Formation and characterization of self-assembled bovine serum albumin nanoparticles as chrysin delivery systems. Colloids and Surfaces B: Biointerfaces 173, 43-51. 10.1016/j.colsurfb.2018.09.046.

Gai, S., Yang, G., Yang, P., He, F., Lin, J., Jin, D., Xing, B., 2018. Recent advances in functional nanomaterials for light–triggered cancer therapy. Nano Today 19, 146-187. 10.1016/j.nantod.2018.02.010.

Geng, S., Zhao, H., Zhan, G., Zhao, Y., Yang, X., 2020. Injectable in Situ Forming Hydrogels of Thermosensitive Polypyrrole Nanoplatforms for Precisely Synergistic Photothermo-Chemotherapy. ACS Applied Materials & Interfaces 12, 7995-8005. 10.1021/acsami.9b22654.

Guo, Y., Luo, J., Tan, S., Otieno, B.O., Zhang, Z., 2013. The applications of Vitamin E TPGS in drug delivery. European Journal of Pharmaceutical Sciences 49, 175-186. 10.1016/j.ejps.2013.02.006.

Hamedi, H., Moradi, S., Hudson, S.M., Tonelli, A.E., 2018. Chitosan based hydrogels and their applications for drug delivery in wound dressings: A review. Carbohydrate Polymers 199, 445-460. 10.1016/j.carbpol.2018.06.114.

Huang, P., Song, H., Zhang, Y., Liu, J., Zhang, J., Wang, W., Liu, J., Li, C., Kong, D., 2016. Bridging the Gap between Macroscale Drug Delivery Systems and Nanomedicines: A Nanoparticle-Assembled Thermosensitive Hydrogel for Peritumoral Chemotherapy. ACS Applied Materials & Interfaces 8, 29323-29333. 10.1021/acsami.6b10416.

Jiang, Y.-W., Gao, G., Hu, P., Liu, J.-B., Guo, Y., Zhang, X., Yu, X.-W., Wu, F.-G., Lu, X., 2020. Palladium nanosheet-knotted injectable hydrogels formed *via* palladium–sulfur bonding for synergistic chemo-photothermal therapy. Nanoscale 12, 210-219. 10.1039/C9NR08454A.

Khafaji, M., Zamani, M., Golizadeh, M., Bavi, O., 2019. Inorganic nanomaterials for chemo/photothermal therapy: a promising horizon on effective cancer treatment. Biophysical Reviews 11, 335-352. 10.1007/s12551-019-00532-3.

Khodaverdi, E., Tafaghodi, M., Ganji, F., Abnoos, K., Naghizadeh, H., 2012. In vitro insulin release from thermosensitive chitosan hydrogel. Aaps Pharmscitech 13, 460-466. 10.1208/s12249-012-9764-9.

Kuang, Y., Zhang, K., Cao, Y., Chen, X., Wang, K., Liu, M., Pei, R., 2017. Hydrophobic IR-780 Dye Encapsulated in cRGD-Conjugated Solid Lipid Nanoparticles for NIR Imaging-Guided Photothermal Therapy. ACS Applied Materials & Interfaces 9, 12217-12226. 10.1021/acsami.6b16705.

Lan, X., She, J., Lin, D.-a., Xu, Y., Li, X., Yang, W.-f., Lui, V.W.Y., Jin, L., Xie, X., Su, Y.-x., 2018. Microneedle-Mediated Delivery of Lipid-Coated Cisplatin Nanoparticles for Efficient and Safe Cancer Therapy. ACS Applied Materials & Interfaces 10, 33060-33069. 10.1021/acsami.8b12926.

Lee, J.H., 2018. Injectable hydrogels delivering therapeutic agents for disease treatment and tissue engineering. Biomaterials Research 22, 1-14. 10.1186/s40824-018-0138-6.

Leitão, M.M., Alves, C.G., de Melo-Diogo, D., Lima-Sousa, R., Moreira, A.F., Correia, I.J., 2020a. Sulfobetaine methacrylate-functionalized graphene oxide-IR780 nanohybrids aimed at improving breast cancer phototherapy. RSC Advances 10, 38621-38630. 10.1039/D0RA07508F

Leitão, M.M., de Melo-Diogo, D., Alves, C.G., Lima-Sousa, R., Correia, I.J., 2020b. Prototypic Heptamethine Cyanine Incorporating Nanomaterials for Cancer Phototheragnostic. Advanced Healthcare Materials 9, 1-19. 10.1002/adhm.201901665.

Li, W., Yang, J., Luo, L., Jiang, M., Qin, B., Yin, H., Zhu, C., Yuan, X., Zhang, J., Luo, Z., 2019a. Targeting photodynamic and photothermal therapy to the endoplasmic reticulum enhances immunogenic cancer cell death. Nature Communications 10, 1-16. 10.1038/s41467-019-11269-8.

Li, Y., Jin, J., Wang, D., Lv, J., Hou, K., Liu, Y., Chen, C., Tang, Z., 2018. Coordination-responsive drug release inside gold nanorod@metal-organic framework core–shell nanostructures for near-infrared-induced synergistic chemo-photothermal therapy. Nano Research 11, 3294-3305. 10.1007/s12274-017-1874-y.

Li, Z., Chen, Y., Yang, Y., Yu, Y., Zhang, Y., Zhu, D., Yu, X., Ouyang, X., Xie, Z., Zhao, Y., 2019b. Recent Advances in Nanomaterials-Based Chemo-Photothermal Combination Therapy for Improving Cancer Treatment. Frontiers in Bioengineering and Biotechnology 7, 1-19. 10.3389/fbioe.2019.00293.

Lima-Sousa, R., de Melo-Diogo, D., Alves, C.G., Cabral, C.S., Miguel, S.P., Mendonça, A.G., Correia, I.J., 2020. Injectable *in situ* forming thermo-responsive graphene based hydrogels for cancer chemo-photothermal therapy and NIR light-enhanced antibacterial applications. Materials Science and Engineering: C 117, 1-8. 10.1016/j.msec.2020.111294.

Lin, S.-Y., Huang, R.-Y., Liao, W.-C., Chuang, C.-C., Chang, C.-W., 2018. Multifunctional PEGylated Albumin/IR780/Iron Oxide Nanocomplexes for Cancer Photothermal Therapy and MR Imaging. Nanotheranostics 2, 106-116. 10.7150/ntno.19379.

Liu, B.-Y., Wu, C., He, X.-Y., Zhuo, R.-X., Cheng, S.-X., 2016. Multi-drug loaded vitamin E-TPGS nanoparticles for synergistic drug delivery to overcome drug resistance in tumor treatment. Science Bulletin 61, 552-560. 10.1007/s11434-016-1039-5

Liu, M., Huang, P., Wang, W., Feng, Z., Zhang, J., Deng, L., Dong, A., 2019a. An injectable nanocomposite hydrogel co-constructed with gold nanorods and paclitaxel-loaded nanoparticles for local chemo-photothermal synergetic cancer therapy. Journal of Materials Chemistry B 7, 2667-2677. 10.1039/C9TB00120D.

Liu, M., Zhang, P., Deng, L., Guo, D., Tan, M., Huang, J., Luo, Y., Cao, Y., Wang, Z., 2019b. IR780-based light-responsive nanocomplexes combining phase transition for enhancing multimodal imaging-guided photothermal therapy. Biomaterials Science 7, 1132-1146. 10.1039/C8BM01524D.

Liu, R., Zhang, H., Zhang, F., Wang, X., Liu, X., Zhang, Y., 2019c. Polydopamine doped reduced graphene oxide/mesoporous silica nanosheets for chemo-photothermal and enhanced photothermal therapy. Materials Science and Engineering: C 96, 138-145. 10.1016/j.msec.2018.10.093.

Liu, W., Zhang, X., Zhou, L., Shang, L., Su, Z., 2019d. Reduced graphene oxide (rGO) hybridized hydrogel as a near-infrared (NIR)/pH dual-responsive platform for combined chemo-photothermal therapy. Journal of Colloid and Interface Science 536, 160-170. 10.1016/j.jcis.2018.10.050.

Ma, Y., Tong, S., Bao, G., Gao, C., Dai, Z., 2013. Indocyanine green loaded SPIO nanoparticles with phospholipid-PEG coating for dual-modal imaging and photothermal therapy. Biomaterials 34, 7706-7714. 10.1016/j.biomaterials.2013.07.007.

Mathew, A.P., Uthaman, S., Cho, K.-H., Cho, C.-S., Park, I.-K., 2018. Injectable hydrogels for delivering biotherapeutic molecules. International Journal of Biological Macromolecules 110, 17-29. 10.1016/j.ijbiomac.2017.11.113.

Merino, S., Martin, C., Kostarelos, K., Prato, M., Vazquez, E., 2015. Nanocomposite hydrogels: 3D polymer–nanoparticle synergies for on-demand drug delivery. ACS nano 9, 4686-4697. 10.1021/acsnano.5b01433.

Miguel, S.P., Ribeiro, M.P., Brancal, H., Coutinho, P., Correia, I.J., 2014. Thermoresponsive chitosan–agarose hydrogel for skin regeneration. Carbohydrate Polymers 111, 366-373. 10.1016/j.carbpol.2014.04.093.

Mó, I., Alves, C.G., de Melo-Diogo, D., Lima-Sousa, R., Correia, I.J., 2020. Assessing the Combinatorial Chemo-Photothermal Therapy Mediated by Sulfobetaine Methacrylate-Functionalized Nanoparticles in 2D and 3D In Vitro Cancer Models. Biotechnology Journal, 2000219. 10.1002/biot.202000219.

Moreira, A.F., Gaspar, V.M., Costa, E.C., de Melo-Diogo, D., Machado, P., Paquete, C.M., Correia, I.J., 2014. Preparation of end-capped pH-sensitive mesoporous silica nanocarriers for on-demand drug delivery. European Journal of Pharmaceutics and Biopharmaceutics 88, 1012-1025. 10.1016/j.ejpb.2014.09.002.

Moreira, A.F., Rodrigues, C.F., Jacinto, T.A., Miguel, S.P., Costa, E.C., Correia, I.J., 2020. Poly (vinyl alcohol)/chitosan layer-by-layer microneedles for cancer chemo-photothermal therapy. International Journal of Pharmaceutics 576, 1-9. 10.1016/j.ijpharm.2019.118907.

Moreira, A.F., Rodrigues, C.F., Reis, C.A., Costa, E.C., Ferreira, P., Correia, I.J., 2018. Development of poly-2-ethyl-2-oxazoline coated gold-core silica shell nanorods for cancer chemo-photothermal therapy. Nanomedicine 13, 2611-2627. 10.2217/nnm-2018-0179.

Nam, J., Son, S., Ochyl, L.J., Kuai, R., Schwendeman, A., Moon, J.J., 2018. Chemo-photothermal therapy combination elicits anti-tumor immunity against advanced metastatic cancer. Nature Communications 9, 1-13. 10.1038/s41467-018-03473-9.

Nguyen, H.N., Ha, P.T., Sao Nguyen, A., Nguyen, D.T., Do, H.D., Thi, Q.N., Thi, M.N.H., 2016. Curcumin as fluorescent probe for directly monitoring in vitro uptake of curcumin combined paclitaxel loaded PLA-TPGS nanoparticles. Advances in Natural Sciences: Nanoscience and Nanotechnology 7, 025001. 10.1088/2043-6262/7/2/025001.

Norouzi, M., Nazari, B., Miller, D.W., 2016. Injectable hydrogel-based drug delivery systems for local cancer therapy. Drug Discovery Today 21, 1835-1849. 10.1016/j.drudis.2016.07.006.

Pais-Silva, C., de Melo-Diogo, D., Correia, I.J., 2017. IR780-loaded TPGS-TOS micelles for breast cancer photodynamic therapy. European Journal of Pharmaceutics and Biopharmaceutics 113, 108-117. 10.1016/j.ejpb.2017.01.002.

Pan, G.-Y., Jia, H.-R., Zhu, Y.-X., Sun, W., Cheng, X.-T., Wu, F.-G., 2018. Cyanine-Containing Polymeric Nanoparticles with Imaging/Therapy-Switchable Capability for Mitochondria-Targeted Cancer Theranostics. ACS Applied Nano Materials 1, 2885-2897. 10.1021/acsanm.8b00527.

Pan, J., Feng, S.-S., 2008. Targeted delivery of paclitaxel using folate-decorated poly(lactide)–vitamin E TPGS nanoparticles. Biomaterials 29, 2663-2672. 10.1016/j.biomaterials.2008.02.020.

Peers, S., Montembault, A., Ladavière, C., 2020. Chitosan hydrogels for sustained drug delivery. Journal of Controlled Release 326, 150-163. 10.1016/j.jconrel.2020.06.012.

Rodrigues, C.F., Alves, C.G., Lima-Sousa, R., Moreira, A.F., de Melo-Diogo, D., Correia, I.J., 2020. Inorganic-based drug delivery systems for cancer therapy, Advances and Avenues in the Development of Novel Carriers for Bioactives and Biological Agents. Elsevier, pp. 283-316.

Samadi, S., Moradkhani, M., Beheshti, H., Irani, M., Aliabadi, M., 2018. Fabrication of chitosan/poly (lactic acid)/graphene oxide/TiO2 composite nanofibrous scaffolds for sustained delivery of doxorubicin and treatment of lung cancer. International Journal of Biological Macromolecules 110, 416-424. 10.1016/j.ijbiomac.2017.08.048.

Shafei, A., El-Bakly, W., Sobhy, A., Wagdy, O., Reda, A., Aboelenin, O., Marzouk, A., El Habak, K., Mostafa, R., Ali, M.A., 2017. A review on the efficacy and toxicity of different doxorubicin nanoparticles for targeted therapy in metastatic breast cancer. Biomedicine & Pharmacotherapy 95, 1209-1218. 10.1016/j.biopha.2017.09.059.

Singh, Y.P., Bhardwaj, N., Mandal, B.B., 2016. Potential of Agarose/Silk Fibroin Blended Hydrogel for in Vitro Cartilage Tissue Engineering. ACS Applied Materials & Interfaces 8, 21236-21249. 10.1021/acsami.6b08285.

Song, J., Zhang, N., Zhang, L., Yi, H., Liu, Y., Li, Y., Li, X., Wu, M., Hao, L., Yang, Z., 2019. IR780-loaded folate-targeted nanoparticles for near-infrared fluorescence image-guided surgery and photothermal therapy in ovarian cancer. International Journal of Nanomedicine 14, 2757-2772. 10.2147/IJN.S203108.

Song, X., Gong, H., Liu, T., Cheng, L., Wang, C., Sun, X., Liang, C., Liu, Z., 2014. J-Aggregates of Organic Dye Molecules Complexed with Iron Oxide Nanoparticles for Imaging-Guided Photothermal Therapy Under 915-nm Light. Small 10, 4362-4370. 10.1002/smll.201401025.

Stern, T., Kaner, I., Zer, N.L., Shoval, H., Dror, D., Manevitch, Z., Chai, L., Brill-Karniely, Y., Benny, O., 2017. Rigidity of polymer micelles affects interactions with tumor cells. Journal of Controlled Release 257, 40-50. 10.1016/j.jconrel.2016.12.013.

Szyma□ska, E., Sosnowska, K., Miltyk, W., Rusak, M., Basa, A., Winnicka, K., 2015. The effect of β-glycerophosphate crosslinking on chitosan cytotoxicity and properties of hydrogels for vaginal application. Polymers 7, 2223-2244. 10.3390/polym7111510.

Ta, H.T., Dass, C.R., Dunstan, D.E., 2008. Injectable chitosan hydrogels for localised cancer therapy. Journal of Controlled Release 126, 205-216. 10.1016/j.jconrel.2007.11.018.

Thomas, R.G., Moon, M.J., Surendran, S.P., Park, H.J., Park, I.-K., Lee, B.-I., Jeong, Y.Y., 2018. MHI-148 Cyanine Dye Conjugated Chitosan Nanomicelle with NIR Light-Trigger Release Property as Cancer Targeting Theranostic Agent. Molecular Imaging and Biology 20, 533-543. 10.1007/s11307-018-1169-z.

Wang, A.Z., Langer, R., Farokhzad, O.C., 2012. Nanoparticle Delivery of Cancer Drugs. Annual Review of Medicine 63, 185-198. 10.1146/annurev-med-040210-162544.

Wang, H., Jiang, L., Wu, H., Zheng, W., Kan, D., Cheng, R., Yan, J., Yu, C., Sun, S.-K., 2019a. Biocompatible Iodine–Starch–Alginate Hydrogel for Tumor Photothermal Therapy. ACS Biomaterials Science & Engineering 5, 3654-3662. 10.1021/acsbiomaterials.9b00280.

Wang, X., Ma, B., Xue, J., Wu, J., Chang, J., Wu, C., 2019b. Defective Black Nano-Titania Thermogels for Cutaneous Tumor-Induced Therapy and Healing. Nano Letters 19, 2138-2147. 10.1021/acs.nanolett.9b00367.

Wilhelm, S., Tavares, A.J., Dai, Q., Ohta, S., Audet, J., Dvorak, H.F., Chan, W.C., 2016. Analysis of nanoparticle delivery to tumours. nature reviews materials 1, 1-12. 10.1038/natrevmats.2016.14.

Xia, F., Niu, J., Hong, Y., Li, C., Cao, W., Wang, L., Hou, W., Liu, Y., Cui, D., 2019. Matrix metallopeptidase 2 targeted delivery of gold nanostars decorated with IR-780 iodide for dual-modal imaging and enhanced photothermal/photodynamic therapy. Acta biomaterialia 89, 289-299. 10.1016/j.actbio.2019.03.008.

Xie, J., Fan, T., Kim, J.H., Xu, Y., Wang, Y., Liang, W., Qiao, L., Wu, Z., Liu, Q., Hu, W., 2020. Emetine-Loaded Black Phosphorus Hydrogel Sensitizes Tumor to Photothermal Therapy through Inhibition of Stress Granule Formation. Advanced Functional Materials 30, 1-8. 10.1002/adfm.202003891.

Xu, J., Gulzar, A., Liu, Y., Bi, H., Gai, S., Liu, B., Yang, D., He, F., Yang, P., 2017. Integration of IR-808 Sensitized Upconversion Nanostructure and MoS2 Nanosheet for 808 nm NIR Light Triggered Phototherapy and Bioimaging. Small 13, 1-13. 10.1002/smll.201701841.

Yang, C., Wu, T., Qi, Y., Zhang, Z., 2018. Recent Advances in the Application of Vitamin E TPGS for Drug Delivery. Theranostics 8, 464-485. 10.7150/thno.22711.

Yang, M., Liu, Y., Hou, W., Zhi, X., Zhang, C., Jiang, X., Pan, F., Yang, Y., Ni, J., Cui, D., 2017. Mitomycin C-treated human-induced pluripotent stem cells as a safe delivery system of gold nanorods for targeted photothermal therapy of gastric cancer. Nanoscale 9, 334-340. 10.1039/C6NR06851K.

Ye, H., Wang, K., Wang, M., Liu, R., Song, H., Li, N., Lu, Q., Zhang, W., Du, Y., Yang, W., 2019. Bioinspired nanoplatelets for chemo-photothermal therapy of breast cancer metastasis inhibition. Biomaterials 206, 1-12. 10.1016/j.biomaterials.2019.03.024.

Zheng, Y., Lan, T., Wei, D., Zhang, G., Hou, G., Yuan, J., Yan, F., Wang, F., Meng, P., Yang, X., 2019a. Coupling the near-infrared fluorescent dye IR-780 with cabazitaxel makes renal cell carcinoma chemotherapy possible. Biomedicine & Pharmacotherapy 116, 1-12. 10.1016/j.biopha.2019.109001.

Zheng, Y., Wang, W., Zhao, J., Wu, C., Ye, C., Huang, M., Wang, S., 2019b. Preparation of injectable temperature-sensitive chitosan-based hydrogel for combined hyperthermia and chemotherapy of colon cancer. Carbohydrate Polymers 222, 1-11. 10.1016/j.carbpol.2019.115039.

Figure Legends

Figure 1 – Characterization of the physicochemical and optical properties of the chitosan-based injectable hydrogels. Schematic representation of the formulation of the injectable *in situ* forming ionotropically crosslinked chitosan hydrogel co-loaded with IR/BPN and DOX/TPN and of its application in chemo-PTT of breast cancer cells (A). Assessment of the swelling behavior of the hydrogels for a period of 48 h (B). Data represents mean ± S.D., n = 5. Evaluation of hydrogels' weight loss in biologically relevant conditions, over a period of 7 days (C). Data represents mean ± S.D., n = 5. Temperature variation curves of the different hydrogel formulations upon NIR laser irradiation (808 nm, 1.7 W cm^{-2}, 10 min) (D). Cumulative release of DOX from IR/BPN+DOX/TPN@Gel during a 48 h period without (w/o NIR) and with (w/ NIR) NIR laser irradiation (808 nm, 1.7 W cm^{-2}, 10 min) (E). Data represents mean ± S.D., n = 3.

Figure 2 – Cytocompatibility of Gel and IR/BPN@Gel. Cell viability of MCF-7 (A) and NHDF (B) cells after their incubation with Gel or IR/BPN@Gel for 24 and 48 h. Data represents mean ± S.D., n = 5. K^- represents the negative control and K^+ represents the positive control.

Figure 3 – Characterization of the phototherapeutic effect mediated by IR/BPN@Gel and IR/BPN+DOX/TPN@Gel. Schematic representation of the PTT and chemo-PTT mediated by IR/BPN@Gel and IR/BPN+DOX/TPN@Gel, respectively (A). Effect of IR/BPN@Gel (3.73 μg mL^{-1} of IR780 equivalents) and IR/BPN+DOX/TPN@Gel (3.29/0.71 μg mL^{-1} of IR780/DOX equivalents) towards MCF-7 cells without (w/o NIR) or with (w/ NIR) NIR laser irradiation (808 nm, 1.7 W cm^{-2}, 10 min) (B). Data represents mean ± S.D., n = 5. (* $p < 0.0001$), n.s. = non-significant.

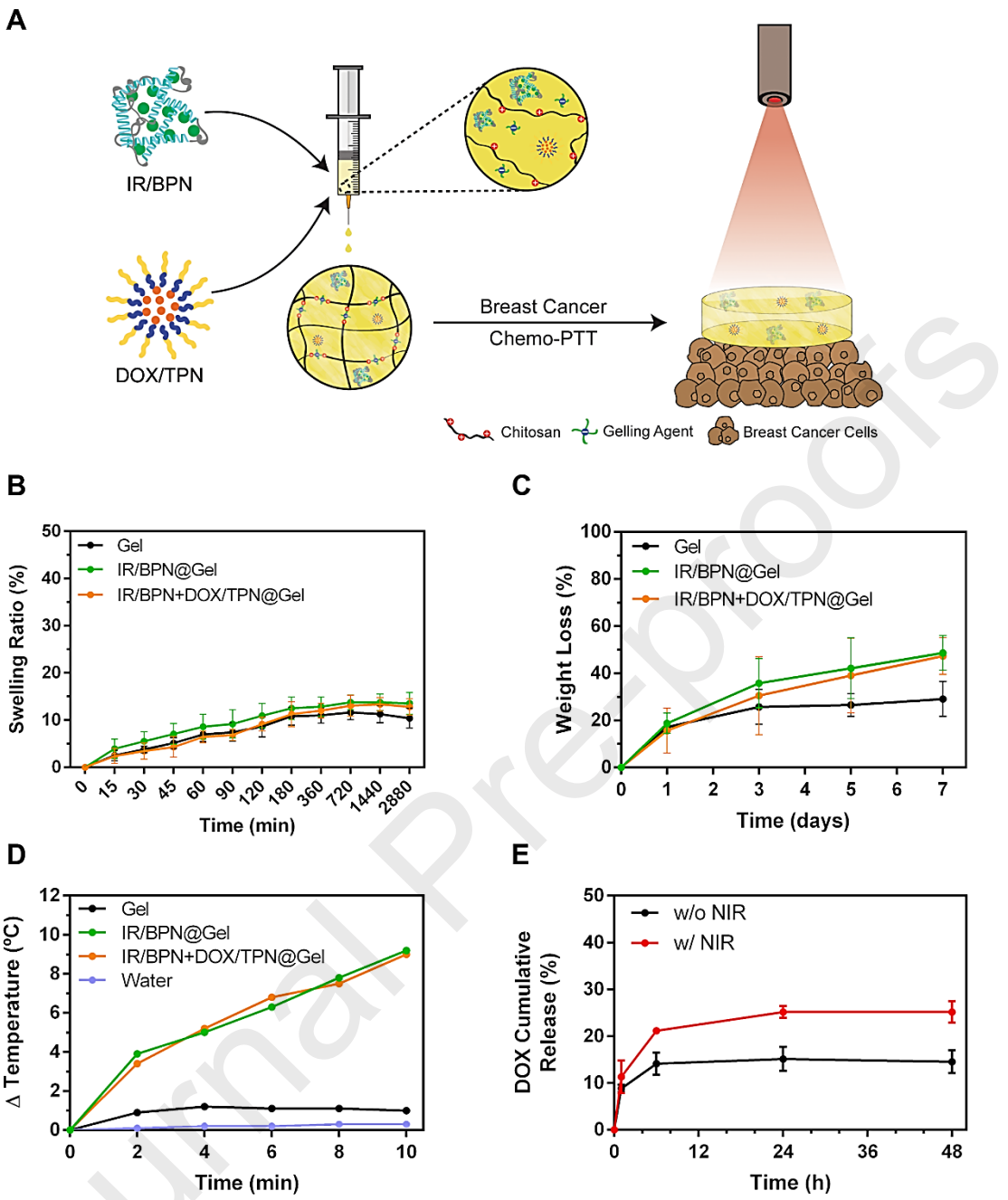

Figure 1

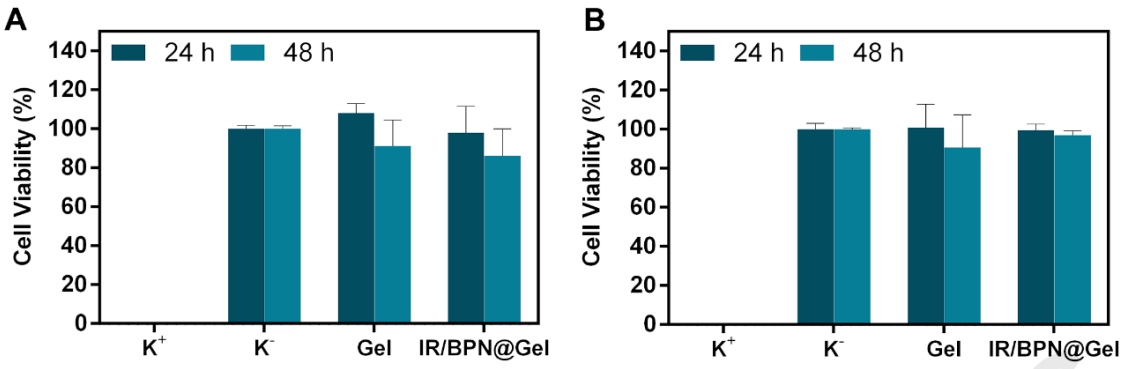

Figure 2

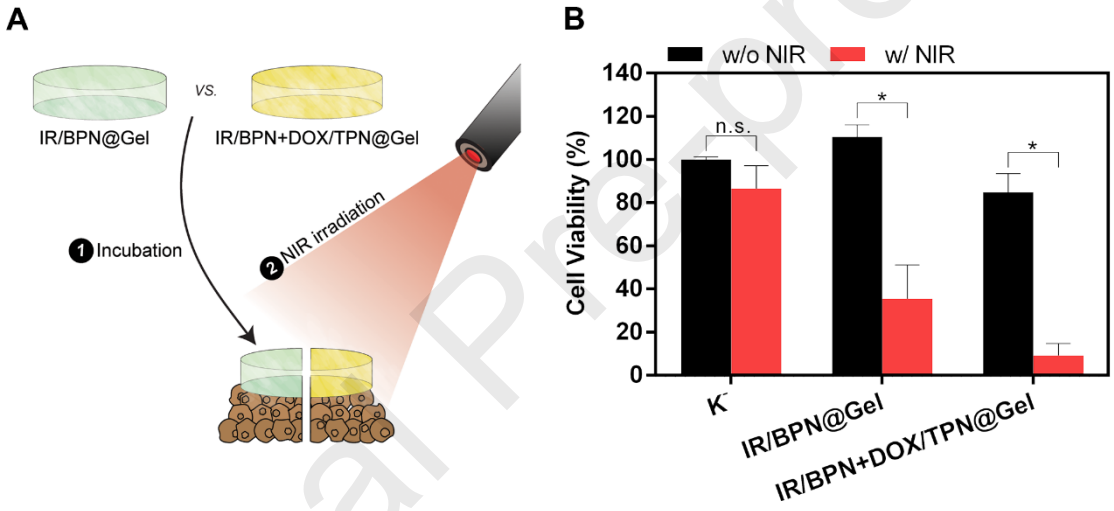

Figure 3

Ivo J. Sabino: Investigation, Formal analysis, Writing – original draft.

Rita Lima-Sousa: Investigation, Supervision, Writing - review & editing.

Cátia G. Alves: Investigation, Supervision, Writing - review & editing.

Bruna L. Melo: Investigation.

André F. Moreira: Writing - review & editing.

Ilídio J. Correia: Project administration, Funding acquisition, Supervision, Writing - review & editing.

Duarte de Melo-Diogo: Conceptualization, Supervision, Writing - review & editing.

Declaration of interests

☒ The authors declare that they have no known competing financial interests or personal relationships that could have appeared to influence the work reported in this paper.

☐The authors declare the following financial interests/personal relationships which may be considered as potential competing interests:

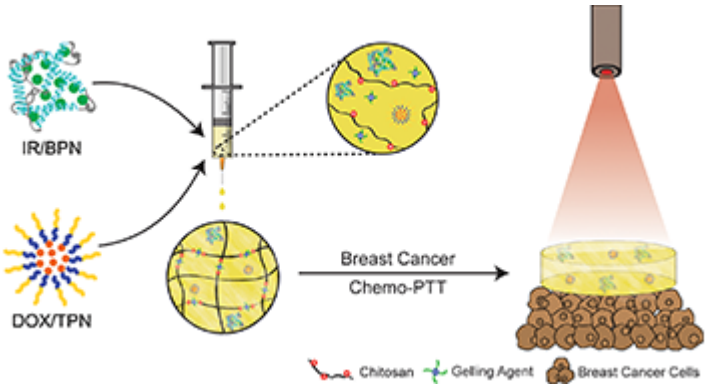

-A novel injectable *in situ* forming chitosan-based hydrogel was prepared for chemo-PTT

-The NIR-responsive hydrogels could produce a temperature increase of about 9 °C

-The NIR-light exposure increased the release of DOX from the hydrogel by 1.7-times

-The chemo-PTT mediated by the hydrogel reduced the viability of cancer cells to 9%